RSC Advances

PAPER

View Article Online
View Journal | View Issue

Cite this: *RSC Adv.*, 2017, **7**, 35875

Capacitive deionization of NaCl solutions with ambient pressure dried carbon aerogel microsphere electrodes†

Xueping Quan,[ab] Zhibing Fu,[b] Lei Yuan,[b] Minglong Zhong,[b] Rui Mi,[b] Xi Yang,[b] Yong Yi*[a] and Chaoyang Wang *[b]

Carbon aerogel (CA) microspheres were pyrolyzed from resorcinol–formaldehyde (RF) organic aerogels, which were prepared by emulsion polymerization of resorcinol and formaldehyde using ambient drying technique. Structural and microstructural characteristics of CA microspheres were investigated by scanning electron microscopy (SEM), Raman spectroscopic techniques and nitrogen adsorption. The SEM images show that the resultant CA microspheres are all fine spherical without cracks. Results of Raman spectroscopy indicate that CA microspheres are mainly formed by amorphous carbon structure with a few graphite carbons. The surface area and porosity analysis prove that the CA microspheres have high specific surface area (910 $m^2\ g^{-1}$), appropriate pore size distribution (PSD) (3–15 nm) and high ratio of mesoporosity (44%). The results of cyclic voltammetry indicate that the CA microspheres have ideal capacitive behavior, and the maximum specific capacitance values of 83 F g^{-1} was measured at a scan rate of 10 mV s^{-1} in 1 M NaCl. These parameters can significantly improve the desalination capacity for the carbon-based electrode materials in capacitive deionization (CDI). The performance of CDI is investigated by different solution concentrations (500–650 mg L^{-1}) and applied voltages (0.8–1.4 V). With the optimum initial NaCl concentration of 500 mg L^{-1} and applied voltage of 1.2 V, the specific salt-adsorption capacity for CA microspheres was found to be 5.62 mg g^{-1}. The electrosorption and electrodesorption procedures displayed the stability and regeneration of CA microsphere electrodes. This preliminary study demonstrated that the CA microsphere electrodes in CDI process can be considered to be an alternative candidate for desalination.

Received 9th May 2017
Accepted 17th June 2017

DOI: 10.1039/c7ra05226j

rsc.li/rsc-advances

1. Introduction

From the last few decades, nearly a seventh of the worldwide population is currently experiencing a serious purified water shortage. To solve this problem, scientists have shown great interest in developing desalination technologies, and following this many desalination methods have been proposed. Among them, the most widely known universal technologies are thermal distillation,[1] reverse osmosis (RO),[2] and electrodialysis.[3] However, these technologies are always energy intensive and expensive, which limit their further application. Compared with conventional processes, the process of capacitive deionization (CDI) is simple, energy-efficient, economical, safe, and clean. These advantages of the CDI process make it the best alternative process in recent years.[4–6]

CDI is a low pressure and no membrane deionization method. In the process of electrosorption, ions can be adsorbed onto the surface of porous electrodes *via* the application of an electric field, to produce deionized water. Then, in the process of electrodesorption, adsorbed ions would be desorbed by reversing the voltages or removing the electric field, resulting in the regeneration of the electrodes.[7] Thus, for CDI, the electrode material is the key component.

Recent efforts have mainly concentrated in novel electrode materials for the CDI process such as carbon aerogel (CA),[4,5] carbon nanotubes (CNT),[8] activated carbon (AC),[9] ordered mesoporous carbon (OMC),[10] graphene[11] and their composites.[12–14] Among them, the specific salt-adsorption capacity (Q) is defined as the salt adsorption amount of per gram activated material and shows the performance of CDI. The value of Q are 3.32 for CNT, 3.68 for AC, and 10.56 mg g^{-1} for OMC, respectively.[15–17] Even though the value of OMC is high, the supramolecular templates of synthesized OMC, such as P123 and CTAB, are often too expensive for bulk production. Accordingly, one of the most promising materials in CDI is CA because of

[a]*School of Materials Science and Engineering, Southwest University of Science and Technology, Mianyang, Sichuan 621000, China. E-mail: yiyong@swust.edu.cn*

[b]*Research Center of Laser Fusion, China Academy of Engineering Physics, Mianyang 621900, China. E-mail: wangchy807@caep.cn*

† Electronic supplementary information (ESI) available: Adsorption isotherms and PSD of CA microspheres under different carbonized temperatures; surface area characteristic of CA microspheres under different carbonized temperatures. See DOI: 10.1039/c7ra05226j

their controllable pore structure, wide range of density variation, high electrical conductivity, relatively low cost, high surface area and great mesopore volume.[18] Pekala *et al.*[18–20] first reported organic aerogel and CA prepared in the resorcinol–formaldehyde (RF) system. Now, researchers always use monolithic CA as electrode materials in CDI.[4,5,21] However, the monolithic CA is generally prepared *via* supercritical drying, and the drying methods demand high pressure and temperature, which restrict their development in the commercial market. Facing this dilemma, more recently, the CA microspheres have drawn more attention as they may offer an attractive alternative to monolith production.[22–25]

The CA microspheres are novel CA materials, which can be synthesized by emulsion polymerization of RF in a slightly basic aqueous solution *via* an ambient drying technology, followed by carbonizing at a high temperature under nitrogen atmosphere.[24–26] There is no solvent exchange process, and hence the cost of production is low and fabrication procedure is uncomplicated as it uses the ambient drying method rather than the traditional supercritical drying. From this aspect, CA microspheres prepared by ambient drying technology pose ideal electrode materials if the pore size distribution (PSD) and available surface area can meet the demand of CDI application. Unfortunately, there have been few reports on the synthesis and properties of CA microspheres used for CDI.

Herein, we first developed CA microspheres with appropriate PSD and high available surface area for CDI *via* ambient drying process. The morphological and structural performances of the CA microspheres have been characterized in detail. The capacitive property of CA microsphere electrodes are further examined by deionization experiments on NaCl solution. The effect of specific salt-adsorption capacity of the CDI systems is also evaluated during the operating conditions.

2. Experimental

2.1 Preparation of CA microspheres

Fig. 1 shows the detailed steps in the synthesis of CA microspheres. As the first step, emulsion polymerization was conducted to synthesize the RF hydrogel microspheres. The molar ratios of resorcinol to sodium carbonate (R/C) and resorcinol to formaldehyde (R/F) were fixed at the value of 500 and 0.5, respectively. The theoretical density of the RF solution was set at 0.6 g mL^{-1}, and distilled water was added as the diluent. Simultaneously, in a three-necked flask, 600 mL industrial white oil and 6.0 g surfactant SPAN80 were added and stirred using a mechanical stirrer at approximately 1000 rpm. Subsequently, the homogeneous RF solution was poured into the industrial white oil containing the surfactant. The solution was stirred for half an hour at 1000 rpm and then the speed of rotation was decelerated to 100 rpm. The emulsions were kept at 333 K with stirring until the dispersive RF microspheres were gelled. The synthesized RF hydrogel microspheres were separated from the industrial white oil through centrifugation and cleaned using dichloromethane. The spheres were then dried at room temperature.

Finally, the CA microspheres were carbonized at 1123, 1223 and 1323 K. The results are shown in Fig. S1 and Table S1 contains the ESI,† which indicates that the optimum carbonization temperature is 1223 K. Therefore, the CA microspheres were obtained by carbonizing at 1223 K for 4 h in an inert atmosphere of nitrogen gas.

2.2 Electrode preparation

The electrodes were obtained by admixing CA microspheres, carbon black and polyvinylidene fluoride (PVDF). PVDF dissolved in *N*-methyl-2-pyrrolidone (NMP) was used as the binder solution. The ratio of CA microspheres, carbon black and PVDF was 7 : 1 : 2 by weight. The slurry of CA microspheres was coated uniformly using a tape coating machine on a titanium plate collector with the size of 10 × 10 cm, and the thickness of the electrode materials was 600 μm. The coated electrodes were dried at 333 K in a vacuum drying oven for 8 h. Electrodes with active material loading of 850 mg were prepared for salt removal experiments.

2.3 Characterization

Scanning electron microscopy (SEM) analysis of CA microspheres was carried out to study their surface morphology (JEOL JSM 5900LV). Raman spectroscopy was performed with laser Raman spectrometer using a laser (514 nm) in the range from 1000 to 2000 cm^{-1} (SPEXCo., USA). Fitting of the spectra was carried out using the Origin software. The PSD and specific surface area of CA microspheres were calculated by analyzing the nitrogen adsorption–desorption isotherms. The system makes use of Brunauer–Emmett–Teller (BET) theory for determining specific surface area and Barrett–Joyner–Halenda (BJH) theory for PSD of mesopores (2–50 nm). The mesopore volume and mesopore surface area of CA microspheres were calculated using the *t*-plot method. The electrosorption behavior of electrodes was evaluated by cyclic voltammetry (CV) measurements in a conventional three electrode cell. The working electrode was formed with the electrode under test. Platinum electrode was used as counter electrode, and a saturated Ag/AgCl electrode was used as the reference electrode. CV were obtained in the potential range from −0.5 to +0.5 V in 1 M NaCl electrolyte.[27,28] The samples were subjected to scan rates of 5, 10 and 20 mV s^{-1}. The specific capacitance expressed in farads per gram, was evaluated using eqn (1):

$$C = \frac{I}{S \cdot m} \quad (1)$$

where I (mA) is the current, S (mV s^{-1}) is applied scan rate, and m is the mass of active material in grams.

2.4 CDI experiments

As shown in Fig. 2(b), CDI experiments were underway in a continuous circulation system including a CDI unit cell, a conductivity meter, peristaltic pump, and a stabilized voltage supply. In this system, the NaCl solution was controlled by the peristaltic pump and flowed through the CDI unit cell. The variation of conductivity of the NaCl solution was measured by

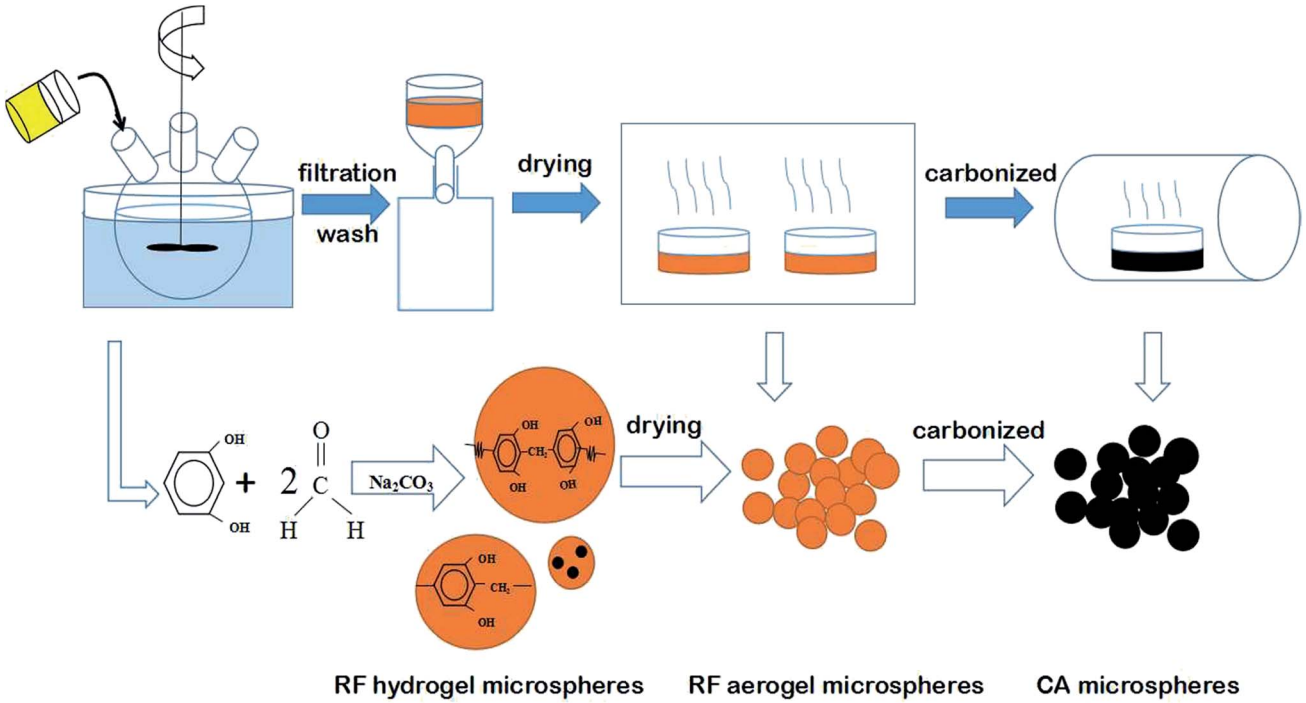

Fig. 1 Diagram of the processing method used for the preparation of CA microspheres.

the conductivity meter. In CDI unit cell, the size of the electrodes was 10 × 10 cm, and the distance between electrodes was 3–5 mm (Fig. 2(a)). In all experiments, 200 mL NaCl solution with different initial concentration was employed as feed solution with a flow rate of 100 mL min^{-1}.

The conductivity linearly increases with the increasing concentration of solution, and thus the concentration of NaCl solution was determined by measuring conductivity of the solution. The calibration curve is shown in Fig. 3. Using this calibration curve, we obtain eqn (2):

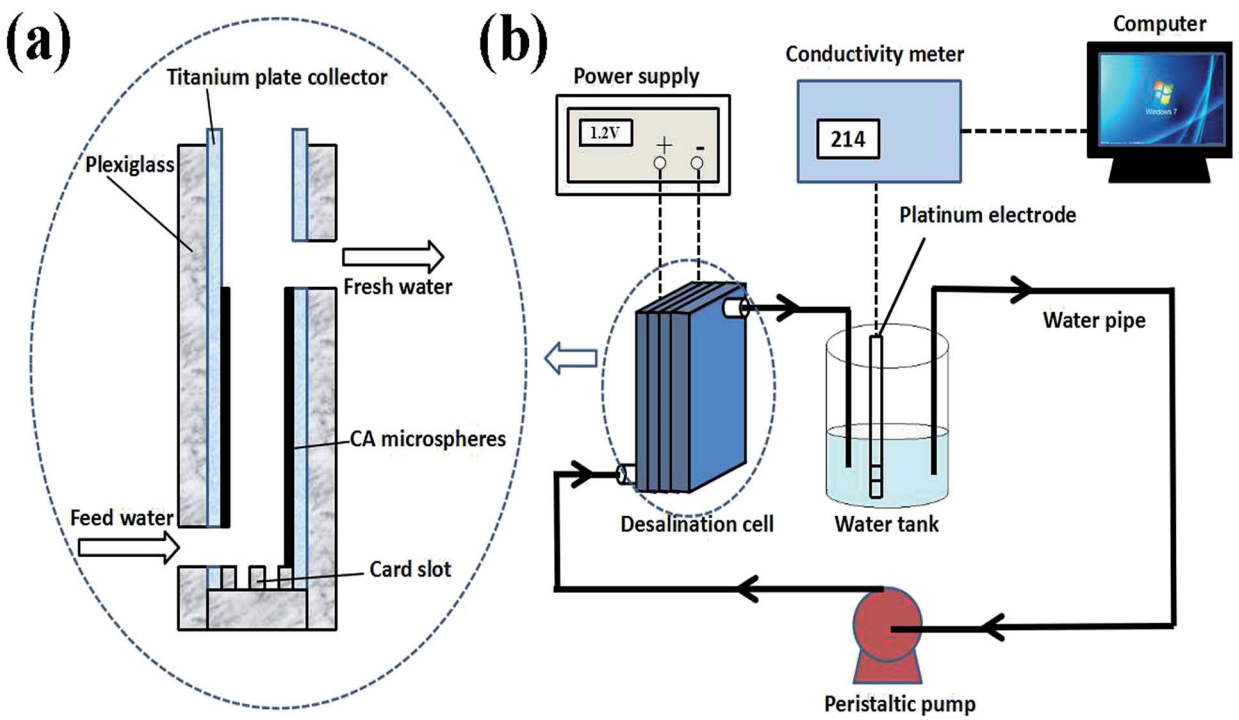

Fig. 2 Diagrammatic sketch of CDI experiment.

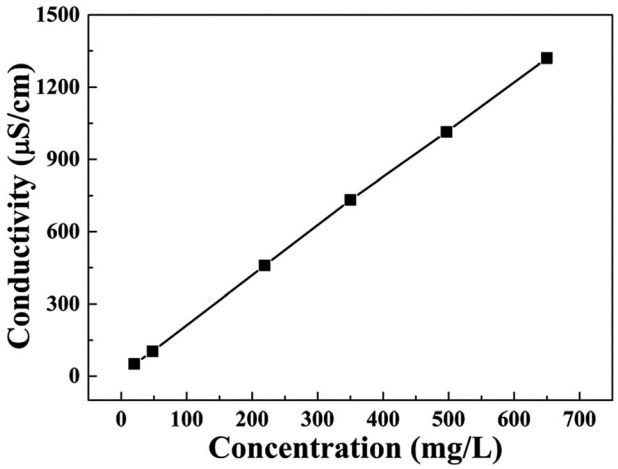

Fig. 3 Calibration curve for ionic conductivity *vs.* NaCl concentration.

$$\text{Cond.} = 12.67 + 2.02C_{\text{NaCl}} \quad (2)$$

where Cond. is the conductivity of solution, and C_{NaCl} is the concentration of NaCl solution. The NaCl concentration can be obtained using the calibration curve made in the experiment. The specific salt-adsorption capacity (Q) is defined as the salt adsorption amount of per gram CA microspheres. It is calculated following equation:[29]

$$Q(\text{mg/g}) = \frac{(C_0 - C_e)V}{m} \quad (3)$$

C_0 and C_e are the initial and equilibrium concentrations, respectively. V is the volume of NaCl solution, m is the quality of active material.[29]

3. Result and discussion

3.1 SEM images of CA microspheres

The SEM images of CA microspheres are shown in Fig. 4. It can be observed that the CA microspheres were all fine spherical and the range of diameters is 1–10 μm (Fig. 4(a)), possessing a smooth surface without cracks and impurity at high magnification (Fig. 4(b)). The resultant CA microspheres have very narrow diameter distribution, which can be attributed to the fact that the microdroplets of the RF aqueous phase are dispersed homogeneously and evenly in the process of the emulsion polymerization. As shown in Fig. 4(c), CA microspheres exhibit porous morphology, and several macropores and large mesopores can be observed at the surface of the microspheres. Fig. 4(d) shows the inner structure of CA microspheres. The CA microspheres are formed by the interconnection of carbon particles. The SEM images indicate that the CA microspheres prepared *via* the ambient pressure drying process have no volume shrinkage. This also shows that using 6.0 g surfactant SPAN80 and the stirring speeds of 1000 rpm, we can successfully synthesize the spherical CA microspheres by the emulsion polymerization and the ambient drying method.[25]

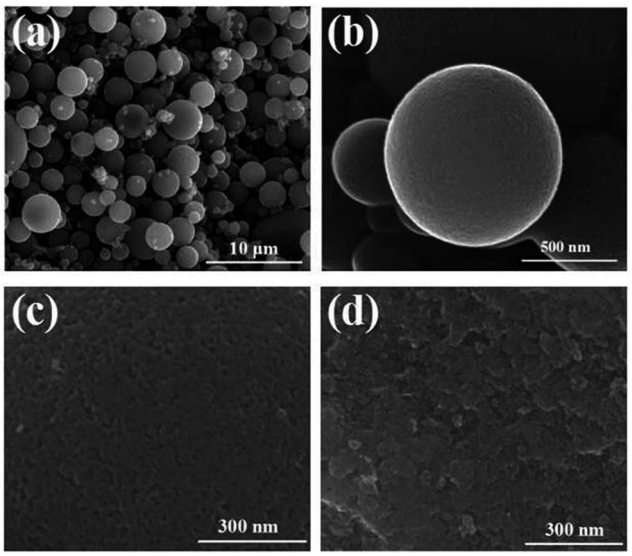

Fig. 4 Scanning electron micrographs of CA microspheres.

3.2 Raman spectra of CA microspheres

Fig. 5 shows the Raman spectrum of CA microspheres. The spectrum is subjected to peak fitting using the software Origin to resolve the curve into 2 Gaussian bands.[30,31] The fitting results of the sample are given in Table 1.

In Fig. 5, there were two broadened and overlapped peaks, the disorder-induced D-band and the ubiquitous G-band, which were located at 1360 and 1580 cm^{-1}, respectively.[32] Generally, the D-band is usually attributed to the lack of long-range translation symmetry in disordered carbons.[33] The G-band corresponds to a tangential stretching E_{2g}, resulting from the 'in plane' displacement of carbon atoms that are strongly coupled in the hexagonal sheets,[32,34] which indicates that there are crystalline graphitic carbon in the CA microspheres. It was found that the D bands of CA microspheres displayed a broad shape and relatively high intensity,

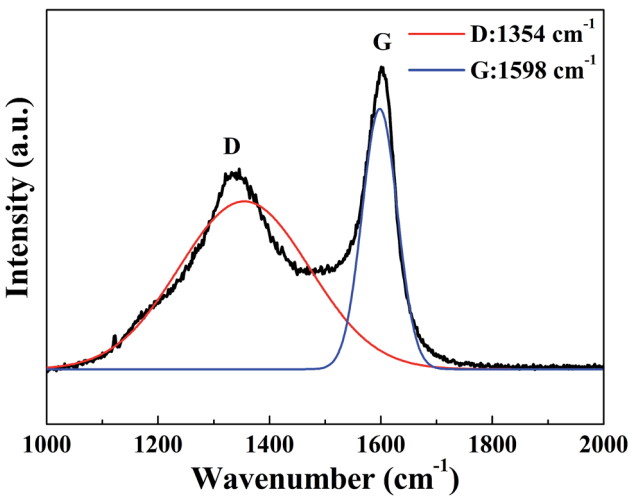

Fig. 5 Raman spectra of CA microspheres.

Table 1 Raman shift and width values for the D and G bands calculated from the fitting spectra

			Band width		
	D shift (cm^{-1})	G shift (cm^{-1})	ΔD (cm^{-1})	ΔG (cm^{-1})	I_D/I_G
Value	1354	1598	223.38	63.27	2.38

indicating the high content of amorphous carbon and some defects in the CA microspheres.

Herein, I_D and I_G represent the peak intensities of the disorder-induced D-band and the ubiquitous G-band, respectively. The in-plane microcrystalline size decreases with an increase in the I_D/I_G.[35] The I_D/I_G also reflects the ratio of disordered carbon and ordered carbon in the CA. Table 1 shows that the I_D/I_G of CA micropheres is consistent with the I_D/I_G ratio of the monolithic CA prepared using supercritical drying,[35] indicating that the crystal structure of CA microspheres prepared by emulsion polymerization and ambient drying technique is mainly amorphous carbon structure with a few graphite carbon.

3.3 Porous properties of CA microspheres

The porous attributes of CA microspheres were characterized by nitrogen sorption tests. Fig. 6 shows the N_2 adsorption–desorption isotherms and the corresponding pore size distribution of CA microspheres, which were calculated using the Barrett–Joyner–Halenda method. Significant adsorption occurred on CA microspheres, and their isotherms belonged to the IV type of the IUPAC classification. There was a hysteresis loop in the curve when the pressure (P/P_0) was larger than 0.4, indicating a large number of mesopores within the sample.

Fig. 6(b) is the mesopore size distributions of the CA microspheres reckoned from the isotherm using the BJH method. The results in Fig. 6(b) demonstrate that the diameters of most pores are below 15 nm. The pore diameter of sample concentrates mainly on around 3.7 nm. The pore size distributions further indicate that there is a little volume shrinkage in the CA microspheres prepared *via* the ambient pressure drying method. More importantly, in the process of CDI experiment, the removal property often depends on the hydrated radii of the sodium ions and chloride ions. The hydrated radii of the sodium ions and chloride ions are 3.58 Å and 3.32 Å, respectively,[36] which are far less than the pore size of the CA microspheres. Hence the CA microspheres satisfy the requirements of CDI.

As shown in Table 2, the BET specific surface area, the pore volume, and the average pore diameter for CA microspheres are 910 $m^2\ g^{-1}$, 0.77 $cm^3\ g^{-1}$, and 3.38 nm, respectively. The N_2 adsorption–desorption isotherms and the pore size distribution curve suggest that the CA microspheres produced *via* ambient drying technique have mesoporous structure, which is similar with the monolithic CA products prepared by traditional supercritical drying. It is worth noting that for the CA microspheres, 44% of the BET specific surface area is attributed to the mesopores (2–50 nm). The high ratio of mesoporosity can significantly improve the desalination performance of the carbon-based electrode materials in CDI.[31] It is clear that the synthesized CA microspheres are propitious to the application of CDI as they have appropriate PSD and high available surface area. Therefore, the CA microspheres synthesized by emulsion polymerization and ambient drying may show great CDI performance when used as electrode material.

3.4 Specific capacitance measurements

The CV curves of the CA microsphere electrodes measured at 5, 10 and 20 mV s^{-1} of scan rate in 1 M NaCl are displayed in Fig. 7. The profiles of curves show quasi-rectangular symmetric and reversible shape in the voltage range from −0.5 to +0.5 V. It is clearly observed that the curves are without any additional oxidation and reduction peaks, suggesting the

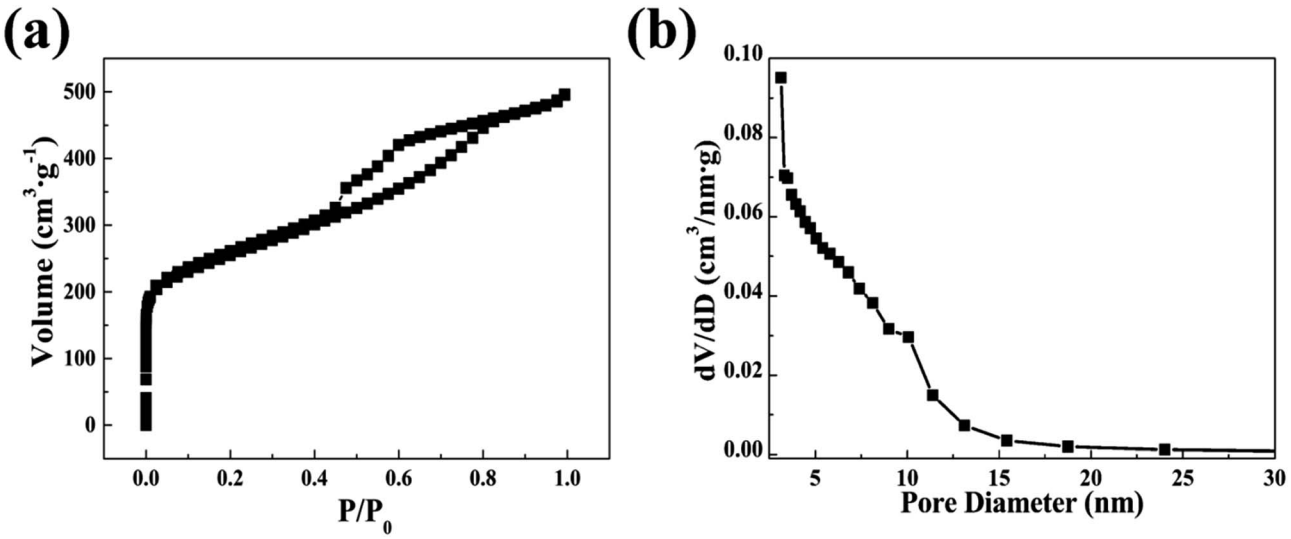

Fig. 6 (a) Adsorption isotherms at 77 K and (b) PSD of CA.

Table 2 Surface area characteristic of CA microspheres

	S_{BET} [a] ($m^2\ g^{-1}$)	S_{meso} [b] ($m^2\ g^{-1}$)	V_{tot} [c] ($cm^3\ g^{-1}$)	V_{meso} [d] ($cm^3\ g^{-1}$)	Average pore diameter (nm)
Value	910	398	0.77	0.60	3.38

[a] BET specific surface area. [b] Mesoporous surface area derived from the t-plot method. [c] Total volume of pores. [d] Volume of mesopores.

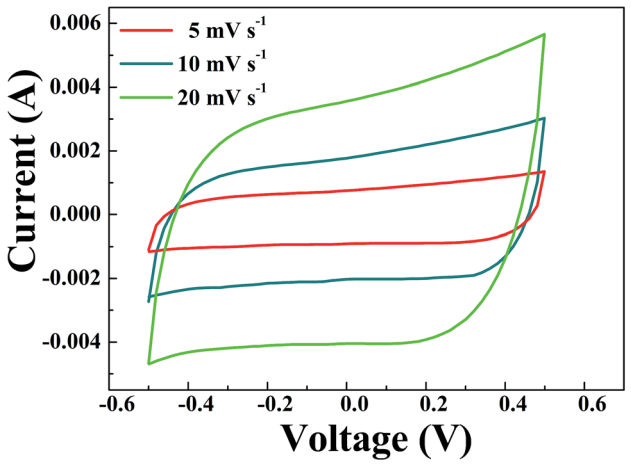

Fig. 7 Cyclic voltammetry curves of CA microspheres electrode in 1 M NaCl solution at several sweep rates.

ideal capacitive behavior. This also means that ions are adsorbed on the surface of electrodes by forming an electric double layer due to coulombic interaction rather than electrochemical reaction.[37] The obtained values of specific capacitance were 83, 75, and 71 F g^{-1} for the scan rate of 5, 10 and 20 mV s^{-1}, respectively. Herein, the capacitance decreases with an increase in the scan rate. This phenomenon can be explained as follows: when the scan rate is slower, ions have more time to be transported into the pores of the materials from solution; thus, the specific capacitance can be more proportional to the specific surface area. The results of the CV curves indicate that CA microspheres with a good adsorption performance may be used as good electrode materials in CDI.

3.5 CDI experiment

In all experiments, the solution temperature was kept at 298 K. The flow rate of the solution was controlled by the peristaltic pump at 100 mL min^{-1}. During each experiment, the NaCl solution passed through the cell without applying voltage until the system reached equilibrium. Furthermore, an expected voltage was applied between the electrodes to reach a new equilibrium. The regeneration was achieved by discharging the cells at 0 V or by reversing the voltage of the electrodes. After that, the CDI unit was washed by deionized water, and the voltage of the CDI unit was reversed to lengthen the life of the CA microsphere electrodes. The important experimental parameters were then investigated. The solution concentration (50–650 mg L^{-1})[38–40] and applied voltage (0.8–1.4 V) were found to have an effect on the CDI systems. Under the operation parameters, the specific salt-adsorption capacity of CA microspheres was calculated. Moreover, the regeneration performance of the electrodes was investigated.

3.5.1 Effect of applied voltage. All experiments were performed with 200 mL NaCl solution (50 mg L^{-1}) flowing through a CDI unit cell with 1.7 g CA microspheres. The applied voltage was in the range from 0.8 to 1.4 V.

Fig. 8 indicates the conductivity variation of the NaCl solution with operating time at various applied voltages (0.8–1.4 V). When the voltage is applied on the system, the solution conductivity decreases with time, and it is said that the NaCl concentration decreases quickly. With an increase in the applied voltage, the ion removal amounts and rates increase. The specific salt-adsorption capacity drop to approximately 1.57 mg g^{-1}, 1.81 mg g^{-1}, 2.15 mg g^{-1} and 2.33 mg g^{-1} at 0.8 V,

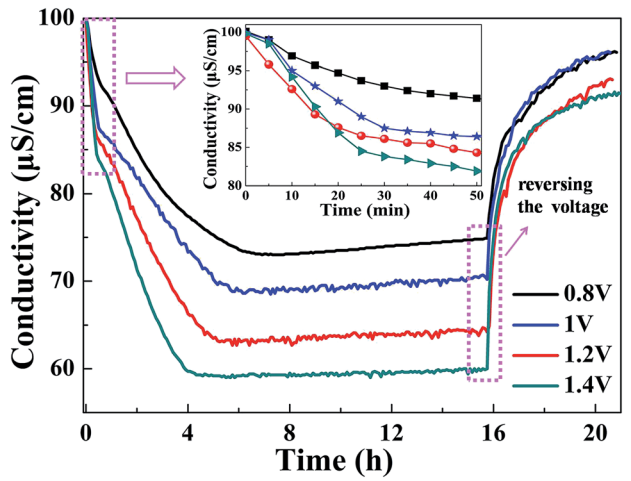

Fig. 8 Conductivity variation of NaCl solution with the various applied voltage.

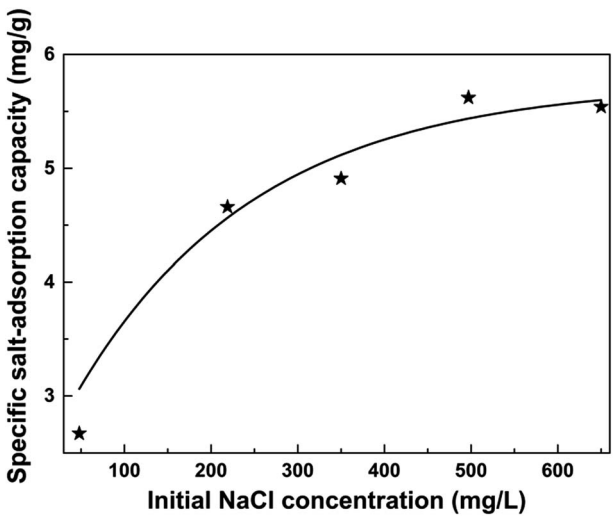

Fig. 9 The specific salt-adsorption capacity variation of NaCl solution with the various initial NaCl concentration.

Table 3 Ion removal characteristics on various NaCl concentrations

NaCl conc. (mg L^{-1})	Conductivity ($\mu S\ cm^{-1}$) Initial	Final	Adsorption time (min)	Q (mg g^{-1})
50	109	63	360	2.67
219	459	379	300	4.66
350	732	648	250	4.91
500	1014	915	90	5.62
650	1320	1225	70	5.54

1 V, 1.2 V and 1.4 V after 6 h, respectively. The adsorption can be maintained for 12 hours. After 16 h of adsorption, 95% Na^+ and Cl^- can be recovered by reversing the voltage. This phenomenon demonstrates that the CA microspheres used as electrode material make the CDI cell exhibit excellent regeneration performance. When the applied voltage is 1.4 V, some bubbles can be observed during the experiment. This is mainly attributed to the fact that the electrochemical decomposition potential of water is 1.23 V. When the applied voltage is larger than 1.23 V, water hydrolyzes partially to produce hydrogen and oxygen. Therefore, the optimum applied voltage for the CDI process was set at 1.2 V.

3.5.2 Effect of NaCl concentration. All experiments were accomplished at an applied voltage of 1.2 V, with 200 mL NaCl solution in the CDI unit cell with 1.7 g CA microspheres. The NaCl concentration varied from 50 to 650 mg L^{-1}.

Fig. 9 shows the variation of specific salt-adsorption capacity with different solution concentrations. In the range of 50–500 mg L^{-1}, the specific salt-adsorption capacity increases with an increase in solution concentration. Nevertheless, when the concentration is 650 mg L^{-1}, the specific salt-adsorption capacity begins to decrease. As shown in Table 3, the specific salt-adsorption capacity is calculated from eqn (2). For the 500 mg L^{-1} NaCl solution, the maximum specific salt-adsorption capacity of the CDI unit system was about 5.62 mg g^{-1}. The value is higher than those of CNT[15] and AC,[16] and is consistent with the reports.[38] The results of the CDI test match well with the above results of nitrogen adsorption and CV test.

3.5.3 Regeneration properties of CA electrodes. The conductivity variation of NaCl solution during adsorption and desorption cycles is shown in Fig. 10. In the desorption process, regeneration of electrodes can be accomplished by two modes, adjusting the voltage at 0.0 V as in Fig. 10(a) and reversing the applied charge as in Fig. 10(b). For both the modes, the absorbed Na^+ and Cl^- ions can be desorbed from the electrodes. The solution conductivity rapidly reaches its initial value. Fig. 10(b) shows that the CDI performances of sample are stable in multiple cycles. Thus, using the CA microspheres as the electrode materials, the electrosorption/electrodesorption procedure is a repeatable and reversible process.

4. Conclusion

Herein, CA microspheres are successfully fabricated *via* pyrolyzing RF organic aerogels, which were synthesized through emulsion polymerization of RF solution, containing sodium carbonate as a catalyst by ambient drying method. The SEM images indicate that all of the prepared CA microspheres were well spherical, possessing a smooth surface without cracks. The obtained Raman spectrum suggests that the CA microspheres prepared by emulsion polymerization and ambient drying technique are mainly formed by amorphous carbon structure with a small amount of graphite carbon. The obtained CA microspheres with average pore diameter of 3.38 nm exhibited the appropriate PSD (3–15 nm) and high available BET specific surface area (910 $m^2\ g^{-1}$). The pore size of CA microspheres fully meets the requirements of CDI. The results of cyclic voltammetry indicate that the CA microspheres have an ideal capacitive behavior, and the maximum specific capacitance of

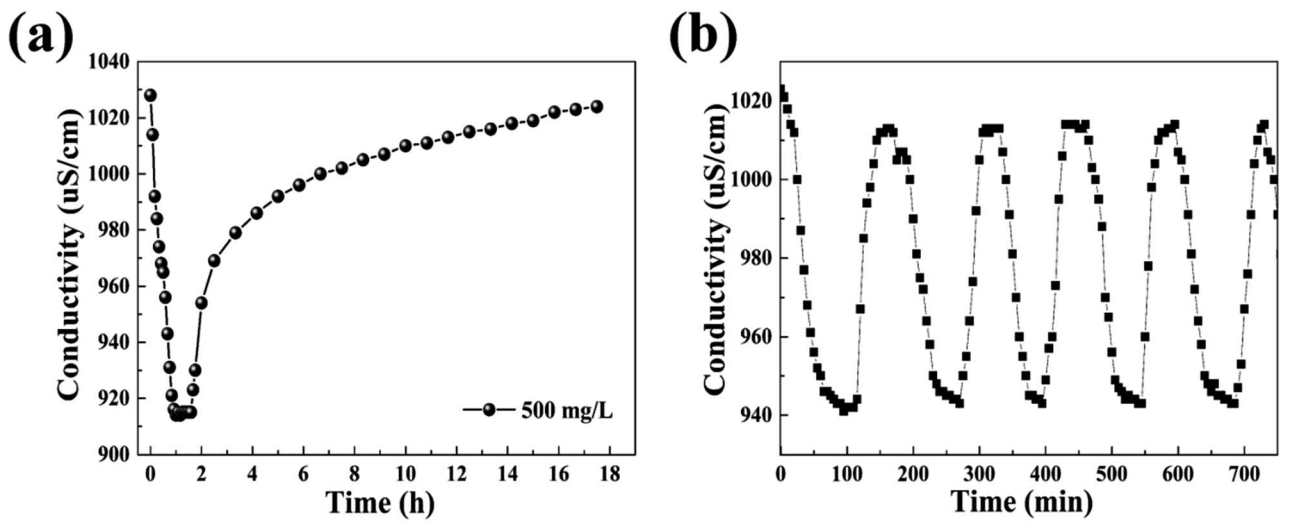

Fig. 10 (a) Conductivity variation of NaCl solution in electrosorption and electrodesorption procedure and (b) sample performance in several circulations.

the electrode reaches 83 F g^{-1} when measured at a scan rate of 10 mV s^{-1} in 1 M NaCl.

The performances of CDI using CA microspheres as electrodes were investigated. The results indicate that the optimum applied voltage and initial NaCl concentration are 1.2 V and 500 mg L^{-1}, respectively. Under optimum experimental parameters, the highest specific salt-adsorption capacity was found to be 5.62 mg g^{-1}. This value is higher than the reported values for related monolithic carbon aerogels. The CA microspheres also exhibited great stability and regeneration as electrodes. This preliminary study demonstrated that the CDI process using CA microsphere electrodes can be considered to be an effective technology for desalination.

Acknowledgements

This study was financially supported by the Science and Technology Project of Sichuan Provincial (2016GZ0235).

References

1 A. J. Morton, I. K. Callister and N. M. Wade, *Desalination*, 1997, **108**, 1–10.
2 V. G. Gude, *Desalin. Water Treat.*, 2011, **36**, 239–260.
3 L. J. Banasiak, T. W. Kruttschnitt and A. I. Schaefer, *Desalination*, 2007, **205**, 38–46.
4 C. J. Gabelich, T. D. Tran and I. H. Suffet, *Environ. Sci. Technol.*, 2002, **36**, 3010–3019.
5 T. Kim and J. Yoon, *RSC Adv.*, 2015, **5**, 1456–1461.
6 R. W. Pekala, J. C. Farmer, C. T. Alviso, T. D. Tran, S. T. Mayer, J. M. Miller and B. Dunn, *J. Non-Cryst. Solids*, 1998, **225**, 74–80.
7 J. C. Farmer, D. V. Fix, G. V. Mack, R. W. Pekala and J. F. Poco, *J. Appl. Electrochem.*, 1996, **26**, 1007–1018.
8 H. Li, Y. Gao, L. Pan, Y. Zhang, Y. Chen and Z. Sun, *Water Res.*, 2008, **42**, 4923–4928.
9 L. Zou, G. Morris and D. Qi, *Desalination*, 2008, **225**, 329–340.
10 C. Tsouris, R. Mayes, J. Kiggans, K. Sharma, S. Yiacoumi, D. DePaoli and S. Dai, *Environ. Sci. Technol.*, 2011, **45**, 10243–10249.
11 Z. Wang, B. Dou, L. Zheng, G. Zhang, Z. Liu and Z. Hao, *Desalination*, 2012, **299**, 96–102.
12 Z. Peng, D. Zhang, L. Shi and T. Yan, *J. Mater. Chem.*, 2012, **22**, 6603–6612.
13 Y. Liu, C. Nie, X. Liu, X. Xu, Z. Sun and L. Pan, *RSC Adv.*, 2015, **5**, 15205–15225.
14 D. Zhang, T. Yan, L. Shi, Z. Peng, X. Wen and J. Zhang, *J. Mater. Chem.*, 2012, **22**, 14696–14704.
15 X. Z. Wang, M. G. Li, Y. W. Chen, R. M. Cheng, S. M. Huang, L. K. Pan and Z. Sun, *Electrochem. Solid-State Lett.*, 2006, **9**, E23–E26.
16 Y.-J. Kim and J.-H. Choi, *Sep. Purif. Technol.*, 2010, **71**, 70–75.
17 F. Duan, Y. Li, H. Cao, Y. Xie and Y. Zhang, *Desalin. Water Treat.*, 2014, **52**, 1388–1395.
18 R. W. Pekala, *J. Mater. Sci.*, 1989, **24**, 3221–3227.
19 R. W. Pekala, *Mater. Res. Soc. Symp. Proc.*, 1990, **171**, 285–292.
20 R. W. Pekala, C. T. Alviso, F. M. Kong and S. S. Hulsey, *J. Non-Cryst. Solids*, 1992, **145**, 90–98.
21 H.-H. Jung, S.-W. Hwang, S.-H. Hyun, L. Kang-Ho and G.-T. Kim, *Desalination*, 2007, **216**, 377–385.
22 C. T. Alviso, R. W. Pekala, J. Gross, X. Lu, R. Caps and J. Fricke, in *Microporous and Macroporous Materials*, ed. R. F. Lobo, J. S. Beck, S. L. Suib, D. R. Corbin, M. E. Davis, L. E. Iton and S. I. Zones, 1996, vol. 431, pp. 521–525.
23 T. Horikawa, J. Hayashi and K. Muroyama, *Carbon*, 2004, **42**, 169–175.
24 N. Liu, S. Zhang, R. Fu, M. S. Dresselhaus and G. Dresselhaus, *J. Appl. Polym. Sci.*, 2007, **104**, 2849–2855.
25 X. Wang, L. Liu, X. Wang, L. Bai, H. Wu, X. Zhang, L. Yi and Q. Chen, *J. Solid State Electrochem.*, 2011, **15**, 643–648.
26 G. Wang, C. Pan, L. Wang, Q. Dong, C. Yu, Z. Zhao and J. Qiu, *Electrochim. Acta*, 2012, **69**, 65–70.
27 Z. Wang, B. Dou, L. Zheng, G. Zhang and Z. Liu, *Desalination*, 2012, **299**, 96–102.
28 Y. Liu, W. Ma, Z. Cheng, J. Xu, R. Wang and X. Gang, *Desalination*, 2013, **326**, 109–114.
29 X. Wang, X. Wang, L. Liu, L. Bai, H. An, L. Zheng and L. Yi, *J. Non-Cryst. Solids*, 2011, **357**, 793–797.
30 H.-B. Zhao, B.-W. Liu, X.-L. Wang, L. Chen, X.-L. Wang and Y.-Z. Wang, *Polymer*, 2014, **55**, 2394–2403.
31 H.-B. Zhao, Z.-B. Fu, H.-B. Chen, M.-L. Zhong and C.-Y. Wang, *ACS Appl. Mater. Interfaces*, 2016, **8**, 1468–1477.
32 F. Tuinstra and J. L. Koenig, *Bull. Am. Phys. Soc.*, 1970, **53**(3), 1126–1130.
33 R. P. Vidano, D. B. Fischbach, L. J. Willis and T. M. Loehr, *Solid State Commun.*, 1981, **39**, 341–344.
34 A. Cuesta, P. Dhamelincourt, J. Laureyns, A. Martinezalonso and J. M. D. Tascon, *Carbon*, 1994, **32**, 1523–1532.
35 A. C. Ferrari and J. Robertson, *Phys. Rev. B: Condens. Matter Mater. Phys.*, 2000, **61**, 14095–14107.
36 C.-L. Yeh, H.-C. Hsi, K.-C. Li and C.-H. Hou, *Desalination*, 2015, **367**, 60–68.
37 M. W. Ryoo, J. H. Kim and G. Seo, *J. Colloid Interface Sci.*, 2003, **264**, 414–419.
38 D. K. Kohli, R. Singh, A. Singh, S. Bhartiya, M. K. Singh and P. K. Gupta, *Desalin. Water Treat.*, 2015, **54**, 2825–2831.
39 H.-H. Jung, S.-W. Hwang, S.-H. Hyun, L. Kang-Ho and G.-T. Kim, *Desalination*, 2007, **216**, 377–385.
40 L. Zou, G. Morris and D. Qi, *Desalination*, 2008, **225**, 329–340.

